



Cite this: *Chem. Commun.*, 2020, **56**, 4672

Received 9th October 2019,  
Accepted 20th February 2020

DOI: 10.1039/c9cc07931a

[rsc.li/chemcomm](http://rsc.li/chemcomm)

Organelle-specific delivery systems are of significant clinical interest. We demonstrate the use of common cyanine dyes Cy3 and Cy5 as vectors for targeting and delivering cargoes to mitochondria in cancer cells. Specifically, conjugation to the dyes can increase cytotoxicity by up to 1000-fold.

Mitochondria are important subcellular organelles for energy production in eukaryotic cells and play critical roles in human health and disease.<sup>1</sup> As dysregulation of mitochondria is associated with a variety of human diseases,<sup>2</sup> vectors delivering therapeutics or biochemical probes to this organelle has significant clinical interest.<sup>3–5</sup> A few molecular entities have been identified as being mitochondria targeting,<sup>4–7</sup> including triphenylphosphonium cations<sup>8,9</sup> and designer peptides.<sup>10,11</sup> It is generally accepted that molecules combining hydrophobic and cationic motifs may exhibit some degree of mitochondrial targeting due to the negative membrane potential (*ca.* –90 to –150 mV in mitochondrial matrix compared to cytosol).<sup>8</sup> Nevertheless, development of chemical entities that can both deliver cargo to mitochondria and report their subcellular location simultaneously is still in its infancy.

Cy3 and Cy5 (Fig. 1a) are commercially available cationic cyanine dyes. They have been commonly used to label molecules for cell fluorescence studies including as a Förster resonance energy transfer (FRET) pair.<sup>12</sup> As a FRET pair, excitation of Cy3 (554 nm) leads to fluorescence emission by Cy5 (666 nm) when the two fluorophores are in close proximity. These dyes are relatively small and hydrophobic yet are highly delocalised cations. There is also evidence suggesting that they tend to locate to mitochondria when incubated with cells at concentrations

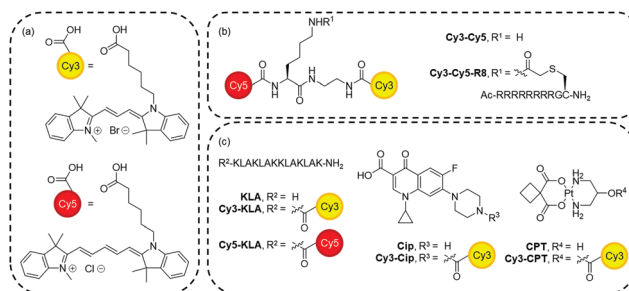


Fig. 1 Structure of compounds used in this study. (a) Cy3 and Cy5. (b) Cy3-Cy5 and Cy3-Cy5-R8. (c) Dye conjugates. Synthetic schemes and procedures are in the ESI.†

over 1  $\mu$ M,<sup>13–18</sup> thus offering them as potential mitochondrial targeting agents. Indeed, other heptamethine dyes have found sporadic usage as mitochondrial probes or delivery vectors.<sup>19–21</sup> However, the full potential of Cy3 and Cy5 for mitochondria targeting and delivery has not been explored. Here, we illustrate that Cy3 and Cy5 are mitochondria targeting as single entities or conjugates and can deliver a variety of structurally diverse molecules (*e.g.* peptide, heterocycle, metallocomplex) to mitochondria to exert cellular effects. Moreover, mitochondrial targeting and delivery capacity is more prominent in cancer cells.

To examine their mitochondria targeting ability, HeLa cells were incubated with 10  $\mu$ M Cy3, Cy5 or Cy3-Cy5 (Fig. 1a and b) followed by live-cell confocal imaging. Cy3-Cy5 was chosen to investigate if having two fluorophores would enhance uptake and targeting effect. This is of interest for designing Cy3-Cy5-based FRET pairs as theranostic targeting vectors. For all three constructs, the observed filamentous staining<sup>22</sup> was highly indicative of mitochondrial accumulation (Fig. 2). The subcellular localisation pattern of these compounds was shown to be concentration independent (Fig. S1, ESI†), and there was no evidence of nuclear localisation (Pearson's correlation coefficients  $< 0.15$ , Fig. 2 and Fig. S2, ESI†) or cytosolic staining. On the other hand, Pearson's coefficients  $> 0.85$  were observed with both Cy3 and Cy5 when cells were subsequently incubated with MitoTracker Green

<sup>a</sup> School of Chemistry, Cardiff University, Cardiff CF10 3AT, UK.  
E-mail: [tsaiy5@cardiff.ac.uk](mailto:tsaiy5@cardiff.ac.uk)

<sup>b</sup> School of Pharmacy and Pharmaceutical Sciences, Cardiff University, Cardiff, CF10 3NB, UK

<sup>c</sup> Institute of Biological Chemistry, Academia Sinica, Taipei 11529, Taiwan

<sup>d</sup> Department of Chemistry, National Taiwan University, Taipei 10617, Taiwan

† Electronic supplementary information (ESI) available: Experimental procedures, characterisation of compounds. See DOI: [10.1039/c9cc07931a](https://doi.org/10.1039/c9cc07931a)

‡ These authors contributed equally.



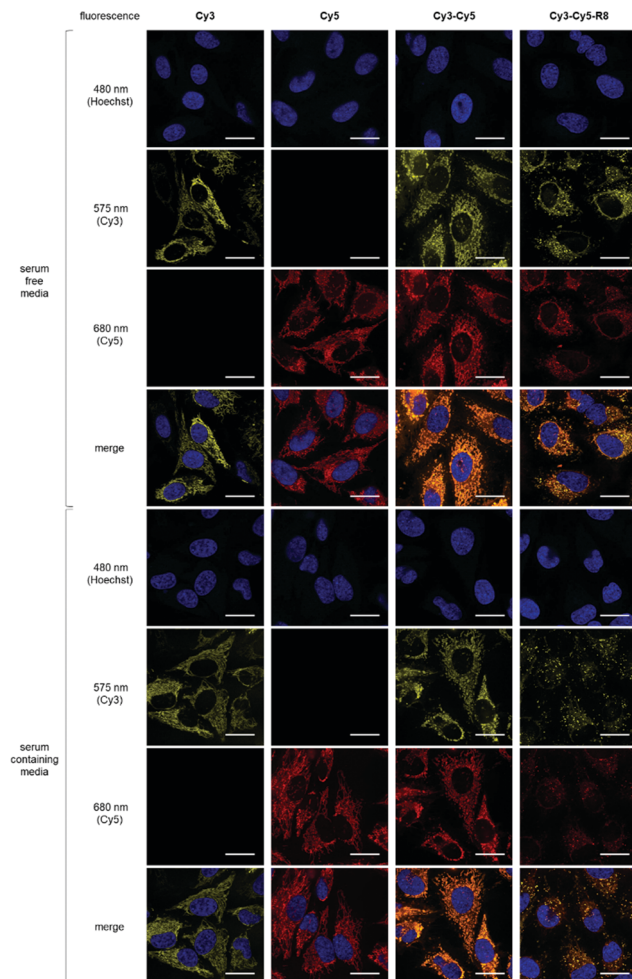


Fig. 2 Representative ( $N = 10$ ) confocal microscopy images of HeLa cells treated with  $10 \mu\text{M}$  of **Cy3**, **Cy5**, **Cy3–Cy5** or **Cy3–Cy5–R8** in the absence or presence of 10% serum at  $37^\circ\text{C}$  for 1 h before imaging. Excitation wavelength for Hoechst, **Cy3**, and **Cy5** is 405, 543, and 633 nm, respectively. Scale bars denote  $25 \mu\text{m}$ .

before imaging (Fig. S3, ESI†), confirming the selective mitochondrial localisation. However, sequential incubation of cells with **Cy3–Cy5** and MitoTracker Green bizarrely showed a different fluorescent pattern when compared to cells that were treated with either molecule alone or as a non-covalent mixture (Fig. S4, ESI†). It is likely that the higher lipophilicity of **Cy3–Cy5** promotes its propensity for aggregation.<sup>23–25</sup> Indeed, lower Pearson's correlation coefficients were also obtained when treating cells with a mixture of **Cy3** and **Cy5** than either **Cy3** or **Cy5** alone with MitoTracker (Fig. S4, ESI†), suggesting hydrophobic interactions between these molecules. Hence, application of **Cy3–Cy5** as a mitochondrial targeting vector is less desirable compared to either **Cy3** or **Cy5**. Nevertheless, it is clear that all constructs preferentially accumulated in mitochondria.

As the mitochondrial membrane potential is the driving force for most cationic, lipophilic mitochondrial targeting molecules,<sup>8</sup> we investigated if the sub-cellular localisation of cyanine dyes depends on the membrane potential. Fixation renders cells permeable to small molecules with a resulting collapse of the

mitochondrial membrane potential. While MitoTracker Green contains functional groups for covalent crosslinking to mitochondria, such functionalities do not exist in **Cy3**. Indeed, little change of fluorescent pattern was observed for MitoTracker Green after fixing the cells with paraformaldehyde,<sup>26</sup> whereas colocalisation of **Cy3** with MitoTracker Green was lost after cell fixation (Fig. 3 and Fig. S5, ESI†). Similarly, when carbonyl cyanide *m*-chlorophenyl hydrazone (CCCP), a known mitochondrial depolarization agent,<sup>15</sup> was added into cells treated with **Cy3**, the filamentous staining rapidly disappeared. Nevertheless, removal of CCCP from the culture media recovered the membrane potential and restored the filamentous mitochondrial staining for **Cy3** after 1 h (Fig. 3). These results indicate that the membrane potential is critical for mitochondrial targeting of the tested cyanine dyes.

A crucial factor in the design of drug delivery vectors is the knowledge of the respective uptake mechanism. Some small molecules can enter cells by passive diffusion, and this was confirmed for **Cy3**, **Cy5** and **Cy3–Cy5** by performing the uptake experiments at  $4^\circ\text{C}$  (Fig. S6 and S7, ESI†), at which no ATP-dependent activity (e.g. endocytosis) takes place. We then examined if cyanine dyes can influence the subcellular localisation and/or the uptake mechanism of a molecule. We and others have explored the potential cell delivery capability of R8, a short cell-penetrating peptide of eight consecutive arginine residues.<sup>27–29</sup> Small-molecule cargoes conjugated to R8 are normally taken up by cells *via* endocytosis at low concentration ( $< 10 \mu\text{M}$ ), but at higher conjugate concentration ( $\geq 10 \mu\text{M}$ ) cytosolic delivery through passive diffusion of the conjugate can also be observed.<sup>30</sup>

Upon conjugation of R8 to cyanine dyes, the behaviour of the resulting **Cy3–Cy5–R8** (Fig. 1b) was examined by confocal microscopy experiments using HeLa cells treated with different concentrations (1, 2.5 or  $10 \mu\text{M}$ ) of **Cy3–Cy5–R8** at either  $4^\circ\text{C}$  or  $37^\circ\text{C}$ . At  $4^\circ\text{C}$ , **Cy3–Cy5–R8** was able to enter cells only at  $10 \mu\text{M}$  but not at  $2.5 \mu\text{M}$  (Fig. S6, ESI†), indicating passive diffusion of

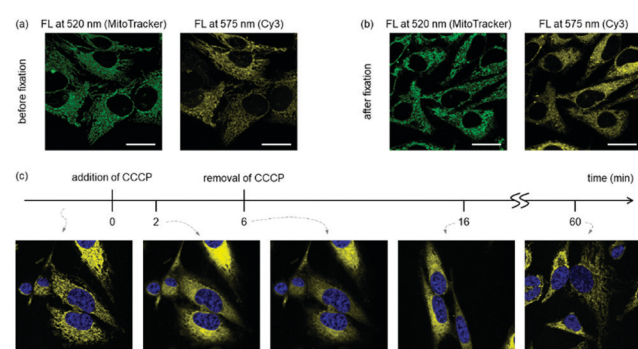


Fig. 3 The membrane potential determines subcellular localisation of **Cy3**. (a and b) HeLa cells were stained with Mito-Tracker Green and **Cy3** and imaged before (a) and after (b) fixation by paraformaldehyde. See Fig. S5 (ESI†) for the correlation analysis. (c) **Cy3**-stained HeLa cells in DMEM containing 10% FBS were treated with  $20 \mu\text{M}$  CCCP for 6 min (from  $t = 0$  to  $t = 6$ ) and washed to remove CCCP. Cells were then incubated in fresh FBS-containing DMEM (from  $t = 6$ ), and images were taken approximately 10 and 55 min afterwards ( $t = 16$  and  $t = 60$ , respectively). Representative ( $N = 2$ ) confocal microscopy images are shown here. FL = Fluorescence.

this conjugate only taking place at 10  $\mu\text{M}$  but not lower concentrations. This observation is in agreement with the literature.<sup>30</sup> While only punctuated fluorescence resembling endolysosomal localisation was observed with 2.5  $\mu\text{M}$  **Cy3-Cy5-R8** at 37 °C (Fig. S7 and S8, ESI†), both punctuate and filamentous fluorescence in the cytoplasm were observed when increasing the conjugate concentration to 10  $\mu\text{M}$  (Fig. 2). However, the fluorescence intensity of **Cy3-Cy5-R8** was influenced by the presence of serum in the culture media unlike the other constructs tested. This is likely due to binding of R8 to serum proteins, thus reducing the extracellular concentration of free conjugates and capacity for cell entry.<sup>31</sup> Nevertheless, the filamentous fluorescence observed with 10  $\mu\text{M}$  **Cy3-Cy5-R8** at 37 °C is indicative of mitochondria accumulation, which is supported by moderate Pearson's correlation coefficients (0.4–0.8) of **Cy3-Cy5-R8** and MitoTracker (Fig. S4, ESI†).

Our results indicate that conjugation to cyanine dyes affected the subcellular localisation of the conjugate but not the uptake mechanism. The mitochondria localisation observed with 10  $\mu\text{M}$  **Cy3-Cy5-R8** at 37 °C most likely resulted from the fraction of **Cy3-Cy5-R8** that first translocated to the cytosol by passive diffusion through the plasma membrane. Once in the cytosol, the conjugate was directed to the mitochondria. The ability of cyanine dyes to alter the subcellular localisation of R8 is unique. It was reported that conjugation of a cell-penetrating peptide with a mitochondrial targeting triphenylphosphonium cation did not cause mitochondrial accumulation of the conjugate.<sup>32</sup> Thus, cationic cyanine dyes may be superior mitochondrial targeting entities than triphenylphosphonium cations.

Having observed and studied the subcellular localisation properties and the cellular uptake mechanisms, we set to evaluate if **Cy3** and **Cy5** can be used to deliver different cargoes to mitochondria to mediate a cellular effect. Three different model cargoes were selected (Fig. 1c) to assess the effect of mitochondrial targeting by conjugation to a cyanine dye. These cargoes are a peptide (**KLA**), a heterocyclic compound (**Cip**), and a metallo-complex (**CPT**). They represent three important classes of drugs in clinical application, and the molecular targets of these cargoes are believed to be in mitochondria.<sup>33–39</sup> **KLAKLAKKLAKLAKLAK (KLA)** is a proapoptotic, antimicrobial peptide.<sup>33,34</sup> Ciprofloxacin (**Cip**) is a fluoroquinolone with antibiotic activity but can also cause damage to mitochondrial DNA, showing cytotoxicity to eukaryotic cells.<sup>35–38</sup> **CPT** is a metal complex and a derivative of carboplatin (a widely used anti-cancer drug) that impairs mitochondrial function and leads to apoptosis.<sup>39</sup> The synthesis of all drug conjugates proved to be rapid and straightforward through simple coupling of the free carboxylic acid of the cyanine dyes. Although conjugates containing both **Cy3** and **Cy5** may enhance their mitochondrial localisation, they may have higher propensity for aggregation. Therefore, we refrained from using conjugates containing two cyanine dyes for delivering mitochondrial-acting cargoes.

To assess the effect of mitochondrial targeting by conjugation to **Cy3**, we first determined the viability of HeLa cells after treatment with either **Cy3**, the unconjugated cargo, a mixture of the unconjugated cargo and **Cy3**, or the respective conjugate. The individual  $\text{EC}_{50}$  values were calculated by curve fitting (Fig. 4 and Fig. S9, ESI†).

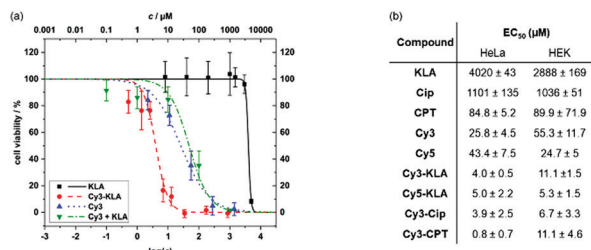


Fig. 4 Toxicity of cyanine dye conjugates in mammalian cells. (a) Representative cell viability curves are shown. Error bars represent the standard deviation of three biological replicates (cells of different passages), and each biological replicate includes three technical replicates (cells of the same passage). (b) The  $\text{EC}_{50}$  values of different molecules and their cyanine dye conjugates were quantified using cell viability assays. The ± values represent the standard error of the curve fitting using Origin 2017.

All conjugates containing a covalent linkage of **Cy3** and the cargo molecule are more cytotoxic than either simple mixtures of **Cy3** and the unconjugated cargo or the cargo alone. Compared to the parent cargo, toxicity increases from 100-fold ( $\text{EC}_{50} = 0.8 \mu\text{M}$  vs. 85  $\mu\text{M}$  for **Cy3-CPT** vs. **CPT**) to 1000-fold were observed ( $\text{EC}_{50} = 4 \mu\text{M}$  vs. 4020  $\mu\text{M}$  for **Cy3-KLA** vs. **KLA**). While **Cy3** alone exhibits cytotoxicity ( $\text{EC}_{50} = 26 \mu\text{M}$ ), a 5- to 30-fold enhancement was observed upon covalent conjugation to the cytotoxic cargo. Confocal microscopy studies of the cargo conjugates were performed to probe the dual functionality of the cyanine dyes to act as mitochondrial targeting/delivery vectors and as diagnostic tools to track cargo localisation (Fig. S10, ESI†). Clear colocalisation of **Cy3-KLA** with MitoTracker Green was observed upon sequential incubation of HeLa cells with MitoTacker and the conjugate (Pearson's correlation coefficient = 0.830), confirming the delivery of **Cy3-KLA** to the mitochondria. Although conjugation of a bioactive molecule to a vector may lead to a decrease in its biological activity<sup>40</sup> (e.g. due to lowering the binding affinity to the cellular target), this does not seem to be the case for **Cy3** conjugation which significantly increases the cytotoxicity (Fig. 4). Nevertheless, it would be interesting to investigate whether using a cleavable linker (e.g. disulphide)<sup>41</sup> that releases the bioactive molecule upon reaching the subcellular target can further enhance the potency of this system.

Moreover, **Cy3** conjugates were found to be more toxic in cancer than non-cancer cells (Fig. S9, ESI†). Specifically,  $\text{EC}_{50}$  values of **Cy3-KLA** are significantly lower ( $p < 0.01$ ) in cancer cell lines (4.0, 1.7, 1.9  $\mu\text{M}$  in HeLa, KB, MCF7) than non-cancer cell lines (11.1, 12.0  $\mu\text{M}$  in HEK, 10T1/2). Up to 10-fold difference in potency was also observed with **Cy3-CPT** ( $\text{EC}_{50} = 0.8 \mu\text{M}$  in HeLa vs. 11.1  $\mu\text{M}$  in HEK). Selectivity in different cells could be due to the more negative mitochondrial membrane potential in cancer cells than non-cancer cells.<sup>42–44</sup> However, HEK and 10T1/2 cells are immortalised and should not be considered as healthy cells. Primary cells or *in vivo* studies are now required to further determine the exact therapeutic window for further translational studies of the conjugates between cancer and healthy cells. Lastly, **Cy5** can also be used as a mitochondrial targeting and delivery vector as it decreases the  $\text{EC}_{50}$  of **KLA** upon forming the conjugated **Cy5-KLA**, demonstrating the general applicability of simple cationic cyanine dyes as targeting entity for bioactive molecule delivery.



In conclusion, our work demonstrated the use of common cyanine dyes as novel vectors for targeting drugs to mitochondria in cancer cells. In addition, due to the fluorescence properties of cyanine dyes, theranostics and novel molecules for photodynamic therapy can be derived and investigated. Nevertheless, our results also highlight how lipophilic cationic dyes as fluorescent labels may influence the cellular fate of labelled compounds in fluorescence studies.

We thank Mr Sanjay G Patel for the initial imaging works in this project and are grateful for the financial support from EPSRC (EP/P511122/1 to A.T. J., Y. H. T.), Wellcome Trust (202056/Z/16/Z to L. Y. P. L.), European Social Fund & Tenovus Cancer Care (Knowledge Economy Skills Scholarship to E. M. M.), and Welsh Government (Life Sciences Research Network Wales Scholarship to D. C.). Information on the original data underpinning the results presented here, including how to access them, can be found in the Cardiff University data catalogue at <http://doi.org/10.17035/d.2020.0102334803>.

## Conflicts of interest

There are no conflicts to declare.

## Notes and references

- 1 M. P. Murphy and R. C. Hartley, *Nat. Rev. Drug Discovery*, 2018, **17**, 865.
- 2 A. H. V. Schapira, *Lancet*, 2012, **379**, 1825.
- 3 P. Gao, W. Pan, N. Li and B. Tang, *Chem. Sci.*, 2019, **10**, 6035.
- 4 H. Zhu, J. Fan, J. Du and X. Peng, *Acc. Chem. Res.*, 2016, **49**, 2115.
- 5 A. Heller, G. Brockhoff and A. Goepferich, *Eur. J. Pharm. Biopharm.*, 2012, **82**, 1.
- 6 S. Rin Jean, D. V. Tulumello, S. P. Wisnovsky, E. K. Lei, M. P. Pereira and S. O. Kelley, *ACS Chem. Biol.*, 2014, **9**, 323.
- 7 R. W. Horobin, S. Trapp and V. Weissig, *J. Controlled Release*, 2007, **121**, 125.
- 8 J. Zielonka, J. Joseph, A. Sikora, M. Hardy, O. Ouari, J. Vasquez-Vivar, G. Cheng, M. Lopez and B. Kalyanaraman, *Chem. Rev.*, 2017, **117**, 10043.
- 9 M. P. Murphy, *Biochim. Biophys. Acta*, 2008, **1777**, 1028.
- 10 S. R. Jean, M. Ahmed, E. K. Lei, S. P. Wisnovsky and S. O. Kelley, *Acc. Chem. Res.*, 2016, **49**, 1893.
- 11 K. K. Maiti, W. S. Lee, T. Takeuchi, C. Watkins, M. Fretz, D. C. Kim, S. Futaki, A. Jones, K. T. Kim and S. K. Chung, *Angew. Chem., Int. Ed.*, 2007, **46**, 5880.
- 12 C. E. Rowland, C. W. Brown, I. L. Medintz and J. B. Delehanty, *Methods Appl. Fluoresc.*, 2015, **3**, 042006.
- 13 I. Negwer, M. Hirsch, S. Kaloyanova, T. Brown, K. Peneva, H. J. Butt, K. Koynov and M. Helm, *ChemBioChem*, 2017, **18**, 1814.
- 14 X. Jia, Q. Chen, Y. Yang, Y. Tang, R. Wang, Y. Xu, W. Zhu and X. Qian, *J. Am. Chem. Soc.*, 2016, **138**, 10778.
- 15 W. J. Rhee and G. Bao, *Nucleic Acids Res.*, 2010, **38**, e109.
- 16 S. Tomcin, G. Baier, K. Landfester and V. Mailänder, *Int. J. Nanomed.*, 2014, **9**, 5471.
- 17 S. Lorenz, S. Tomcin and V. Mailänder, *Microsc. Microanal.*, 2011, **17**, 440.
- 18 N. Chuard, K. Fujisawa, P. Morelli, J. Saarbach, N. Winssinger, P. Metrangolo, G. Resnati, N. Sakai and S. Matile, *J. Am. Chem. Soc.*, 2016, **138**, 11264.
- 19 S. Luo, X. Tan, S. Fang, Y. Wang, T. Liu, X. Wang, Y. Yuan, H. Sun, Q. Qi and C. Shi, *Adv. Funct. Mater.*, 2016, **26**, 2826.
- 20 Y. Liu, J. Zhou, L. Wang, X. Hu, X. Liu, M. Liu, Z. Cao, D. Shangguan and W. Tan, *J. Am. Chem. Soc.*, 2016, **138**, 12368.
- 21 S. M. Usama, B. Zhao and K. Burgess, *Bioconjugate Chem.*, 2019, **30**, 1175.
- 22 R. Ban-Ishihara, T. Ishihara, N. Sasaki, K. Mihara and N. Ishihara, *Proc. Natl. Acad. Sci. U. S. A.*, 2013, **110**, 11863.
- 23 J. Kang, O. Kaczmarek, J. Liebscher and L. Dähne, *Int. J. Polym. Sci.*, 2010, **2010**, 1.
- 24 N. Fu, Y. Xiong and T. C. Squier, *J. Am. Chem. Soc.*, 2012, **134**, 18530.
- 25 L. I. Markova, V. L. Malinovskii, L. D. Patsenker and R. Häner, *Chem. Commun.*, 2013, **49**, 5298.
- 26 B. Chazotte, *Cold Spring Harb. Protoc.*, 2011, **2011**, 990.
- 27 S. G. Patel, E. J. Sayers, L. He, R. Narayan, T. L. Williams, E. M. Mills, R. K. Allemann, L. Y. P. Luk, A. T. Jones and Y. H. Tsai, *Sci. Rep.*, 2019, **9**, 6298.
- 28 M. Gallo, S. Defaus and D. Andreu, *Arch. Biochem. Biophys.*, 2019, **661**, 74.
- 29 C. P. Cerrato, K. Künnapuu and Ü. Langel, *Expert Opin. Drug Delivery*, 2017, **14**, 245.
- 30 A. T. Jones and E. J. Sayers, *J. Controlled Release*, 2012, **161**, 582.
- 31 M. Kosuge, T. Takeuchi, I. Nakase, A. T. Jones and S. Futaki, *Bioconjugate Chem.*, 2008, **19**, 656.
- 32 M. F. Ross, A. Filipovska, R. A. Smith, M. J. Gait and M. P. Murphy, *Biochem. J.*, 2004, **383**, 457.
- 33 B. Law, L. Quinti, Y. Choi, R. Weissleder and C. H. Tung, *Mol. Cancer Ther.*, 2006, **5**, 1944.
- 34 Z. M. Jeffrey, C. Mai, S.-H. Kim, B. Ng and P. D. Robbins, *Cancer Res.*, 2001, **61**, 7709.
- 35 J. W. Lawrence, D. C. Claire, V. Weissig and T. C. Rowe, *Mol. Pharmacol.*, 1996, **50**, 1178.
- 36 J. Azéma, B. Guidetti, J. Dewelle, B. Le Calve, T. Mijatovic, A. Korolyov, J. Vaysse, M. Malet-Martino, R. Martino and R. Kiss, *Bioorg. Med. Chem.*, 2009, **17**, 5396.
- 37 S. Kalghatgi, C. S. Spina, J. C. Costello, M. Liesa, J. R. Morones-Ramirez, S. Slomovic, A. Molina, O. S. Shirihai and J. J. Collins, *Sci. Transl. Med.*, 2013, **5**, 192ra85.
- 38 A. Hangas, K. Aasumets, N. J. Kekäläinen, M. Paloheinä, J. L. Pohjoismäki, J. M. Gerhold and S. Goffart, *Nucleic Acids Res.*, 2018, **46**, 9625.
- 39 V. Reshetnikov, S. Daum, C. Janko, W. Karawacka, R. Tietze, C. Alexiou, S. Paryzhak, T. Dumych, R. Bilyy, P. Tripal, B. Schmid, R. Palmisano and A. Mokhir, *Angew. Chem., Int. Ed.*, 2018, **57**, 11943.
- 40 Y.-H. Tsai, S. Essig, J. J. James, K. Lang and J. W. Chin, *Nat. Chem.*, 2015, **7**, 554.
- 41 E. K. Lei and S. O. Kelley, *J. Am. Chem. Soc.*, 2017, **139**, 9455.
- 42 S. Kim, L. Palanikumar, H. Choi, M. T. Jeena, C. Kim and J. H. Ryu, *Chem. Sci.*, 2018, **9**, 2474.
- 43 S. Marrache and S. Dhar, *Chem. Sci.*, 2015, **6**, 1832.
- 44 C. J. Zhang, Q. Hu, G. Feng, R. Zhang, Y. Yuan, X. Lu and B. Liu, *Chem. Sci.*, 2015, **6**, 4580.

